Performance of Cell-Free Massive MIMO Networks under Rayleigh and Rician fading

Thaissa T. R. Ueoka, Daynara D. Souza, Marx M. M. Freitas, André M. Cavalcante, and João C. W. A. Costa

***Abstract*— This work investigates the impact of different channel fadings on the favorable propagation, channel hardening, and spectral efficiency of cell-free massive multiple-input multiple-output (MIMO) systems. The analyzes consider both line-of-sight (LOS) and non-LOS (NLOS) channels in indoor and outdoor environments. Specifically, the channel may be subject to correlated and uncorrelated Rayleigh or Rician fading. The results indicate that cell-free systems can present more hardening and spectral efficiency when the channel behaves like a Rician fading. On the other hand, they may benefit from more favorable propagation in Rayleigh fading channels.**

***Keywords*— Cell-free massive MIMO, Channel hardening, Favorable propagation, Rayleigh and Rician fading.**

I. Introduction

Cell-free (CF) massive multiple-input multiple-output (MIMO) networks consist of a large number of access points (APs) distributed in the coverage area that cooperates to serve the user equipment (UE). In these systems, channel hardening (CHD) [1] is essential since it allows UEs to use statistical channel state information (CSI) to decode their data. Another important phenomenon is favorable propagation (FVP) [1], defined as mutual orthogonality between channel vectors from different UEs. This property makes it easier for the APs to mitigate interference between UEs through combining and precoding techniques [1]. These phenomena have different outcomes depending on channel models, precoding schemes, and propagation scenarios. Therefore, it is necessary to assess the impact of these considerations in the CF scenario.

II. Channel Models

The channels are modeled considering a network composed of L APs, each one equipped with N antennas, serving K UEs. First, only the line-of-sight (LOS) component is considered, which is the shortest path between the AP and UE. The APs are considered to be equipped with half-wavelength-spaced uniform linear arrays (ULAs). Thus, the LOS channel between AP l and UE k can be written as

$$\mathbf{h}_{kl}^{\mathrm{LOS}} = \sqrt{\beta_{kl}} \left[1, e^{-\mathrm{j}\pi \sin(\varphi_{kl})}, \cdots, e^{-\mathrm{j}(N-1)\pi \sin(\varphi_{kl})}\right]^{\mathrm{T}} e^{j\theta_{kl}}, \quad (1)$$

where φ_{kl} is the angle-of-arrival (AoA) and β_{kl} is the large-scale fading gain, including path loss and shadowing. Due to the UEs' mobility, random phase shifts $\theta_{kl} \sim \mathcal{U}[0, 2\pi)$ occur.

Thaissa T. R. Ueoka[1], Daynara D. Souza[1], Marx M. M. Freitas[1], André M. Cavalcante[2] and João C. W. A. Costa[1]. [1]Applied Electromagnetism Laboratory, Federal University of Pará - UFPA, Belém, Brazil, [2]Ericsson Research, Ericsson Telecomunicações S.A., Indaiatuba, Brazil. E-mails: thaissa.ueoka@itec.ufpa.br; daynara@ufpa.br; marx@ufpa.br; andre.mendes.cavalcante@ericsson.com; jweyl@ufpa.br. This work was supported by Ericsson Telecomunicações S.A, CNPq and CAPES.

Second, only the multipath components non-line-of-sight (NLOS) are considered, and LOS is blocked, showing a Rayleigh distribution. For uncorrelated Rayleigh, the channel follows a complex Gaussian distribution, and there is no correlation between the different antenna elements, whereas there is for correlated Rayleigh fading. In this regard, it is considered that the channel vector between the UE k and AP l undergoes an independent uncorrelated or correlated Rayleigh fading realization, which is given by

$$\mathbf{h}_{kl}^{\mathrm{NLOS(uncor)}} = \sqrt{\beta_{kl}}\, \mathbf{g}_{kl}, \quad \mathbf{h}_{kl}^{\mathrm{NLOS(cor)}} = \sqrt{\mathbf{R}_{kl}}\, \mathbf{g}_{kl}, \quad (2)$$

where $\mathbf{g}_{kl} \in \mathbb{C}^{N\times 1}$ is composed of elements that are independent and identically distributed (i.i.d.) complex Gaussian $\mathcal{N}_{\mathbb{C}}(0, 1)$ random variables (RVs). The correlation matrix $\mathbf{R}_{kl}$ is computed following the Gaussian local scattering spatial correlation model presented in [1], with $\beta_{kl} = \mathrm{tr}\{\mathbf{R}_{kl}\}/N$ being the large-scale gain.

To model a scenario that considers the possibility of both LOS and NLOS propagation components, the channel vector $\mathbf{h}_{kl} \in \mathbb{C}^{N\times 1}$ between the AP l and UE k undergoes independent Rician fading, being defined as [2]

$$\mathbf{h}_{kl} = \sqrt{\frac{\kappa_{kl}}{1+\kappa_{kl}}}\mathbf{h}_{kl}^{\mathrm{LOS}} + \sqrt{\frac{1}{1+\kappa_{kl}}}\mathbf{h}_{kl}^{\mathrm{NLOS}}, \quad (3)$$

where the first term corresponds to the deterministic LOS component, and the second term is the random component from NLOS propagation. For uncorrelated Rician fading, $\mathbf{h}_{kl}^{\mathrm{NLOS}}$ is given by the first equation in (2), while the second equation is used for correlated Rician fading. The Rician factor κ_{kl} represents the power ratio between the LOS and NLOS components, defined as $\kappa_{kl} = p_{\mathrm{LOS}}/(1 - p_{\mathrm{LOS}})$, where p_{LOS} is the probability of the LOS component exists, being equal to zero for propagation links that are only NLOS [3].

III. Results

The propagation models and LOS probability adopted in this paper follow the 3GPP TR 38.901. For indoor scenarios, it is considered the indoor hotspot open office (InH-open) and the urban micro (UMi) for the outdoor. It is considered that there are 20 UEs, 4 antennas per AP, and 10 mutually orthogonal uplink (UL) pilot sequences in the network. The UEs and APs are uniformly distributed in the coverage area. The carrier frequency is 3.5 GHz with 100 MHz of bandwidth. The noise figure is 8 dB, the UL power is 22 dBm for each UE, and the other simulation parameters are given in Table I [1].

Fig. 1 shows the cumulative distribution function (CDF) of the downlink (DL) spectral efficiency (SE) in CF systems for different channel fadings in indoor environments when the

TABLE I: Downlink parameters for simulation.

PARAMETER	INDOOR	OUTDOOR
Number of APs	20	100
Coherence block samples	3750	200
AP and UE heights	3 m, 1.65 m	11.65 m, 1.65 m
AP total Tx power	15 dBm	23 dBm
Coverage area	100m × 100m	1000m × 1000m

maximum ratio (MR) precoding is applied. In Fig. 1a, the best performance is achieved in the Rayleigh channel, experiencing the smallest mutual interference from the simultaneous transmission of several data streams to the UEs. This happens because the information arrives from diverse channel paths, mitigating the interference among them. The Rician channel also presents reasonable levels of FVP, similar to the Rayleigh. On the other hand, to the LOS channels present FVP, the UEs' AoAs need to be different. One can note that on CF, approximately 65% of cases have better FVP than on cellular systems under uncorrelated Rayleigh assuming a base station with the same number of antennas [4].

In Fig. 1b, the LOS channel achieves the best CHD degree, presenting slight variations and better signal stability because it is an almost deterministic channel without multiple paths. The Rician channel has a better CHD than Rayleigh for having the deterministic LOS component. The uncorrelated channel improve CHD by having better channel diversity. That is, one path compensates for the other, different from the correlated ones. Moreover, CF has a worse level of CHD than cellular in most cases, because different APs locations cause more variation in gains. In Fig. 1c, the SE behavior can be explained by the relationship between CHD and FVP. It is observed that the Rician channels achieve higher SEs than Rayleigh ones because they provide more hardening while reaching similar levels of FVP.

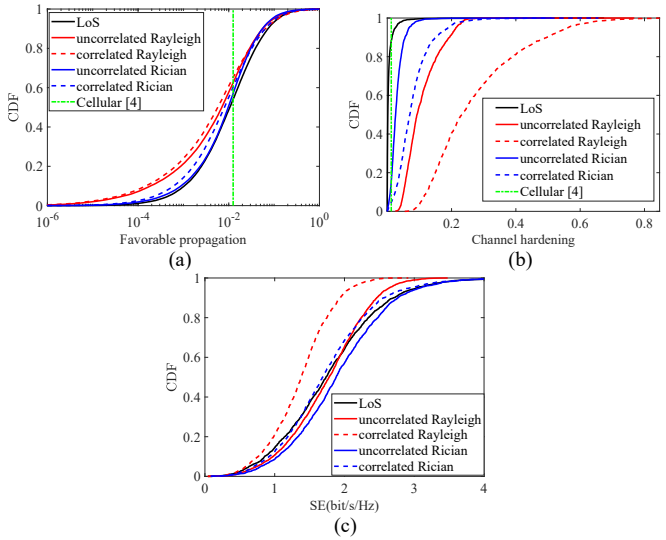

Fig. 1: FVP, CHD and SE of the LOS, Rayleigh and Rician channels in the indoor scenario.

Fig. 2a analyses the performance of CF systems under MR, local partial minimum mean square error (LP-MMSE), and partial minimum mean square error (P-MMSE) precoding schemes [1] in the correlated Rician channel. The best precoding is the one that can mitigate the most interference, which is the case of LP-MMSE and P-MMSE. The comparisons are performed for the cases where the UEs have access to the perfect CSI (pCSI), or the statistical CSI, which exploits the imperfect knowledge of the channel to decode data. One can note that LP-MMSE and P-MMSE outperform MR. For example, the SE of P-MMSE is almost double of MR in the 50$^{\text{th}}$ percentile, but at the cost of approximately 10^5 complex multiplications for combining vector computation, while none is needed for MR [1]. The choice of precoding relies on the compromise between performance and computational cost.

Fig. 2b evaluates the impact of the Rician fading channel in indoor and outdoor scenarios. One can note that the pCSI brings only slight improvements in the SE in indoor environments. However, a significant difference is observed in outdoor scenarios, indicating that the CHD is smaller. The difference between the scenarios is due to the LOS component. As the LOS component is less likely to be present in larger coverage areas, CHD is less pronounced in outdoor scenarios.

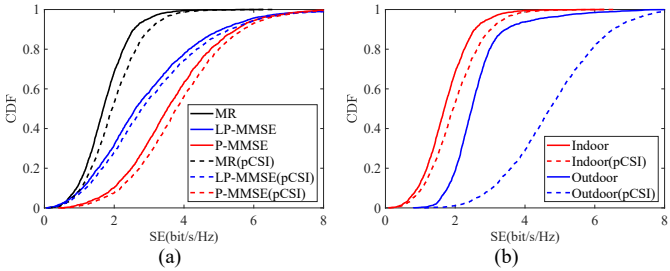

Fig. 2: Rician channel. (a) Different precoders in the indoor scenario. (b) SE for MR in the indoor and outdoor scenarios.

IV. Conclusions

This work has investigated the performance of FVP, CHD, and SE for Rician and Rayleigh channels. The results have indicated that CF systems achieve higher SE when the channel behaves as a Rician fading. In these scenarios, the system has more hardening than in Rayleigh fading channels while reaching similar FVP levels. The results also indicate that the statistical CSI is unreliable in outdoor scenarios. The low degrees of CHD in outdoor environments make CF systems suffer from poor SE performance. Therefore, it is more recommendable to adopt alternative DL channel estimation methods, such as blind estimation or DL pilot-based to improve SE in outdoor scenarios.

References

[1] Ö. Demir, E. Björnson, and L. Sanguinetti, *Foundations of User-Centric Cell-Free Massive MIMO*. Foundations and Trends in Signal Processing Series, Now Publishers, 2021.

[2] O. Ozdogan, E. Bjornson, and E. G. Larsson, "Massive MIMO with spatially correlated rician fading channels," *IEEE Transactions on Communications*, vol. 67, no. 5, pp. 3234–3250, May 2019.

[3] C. D'Andrea, A. Garcia-Rodriguez, G. Geraci, L. Giordano, and S. Buzzi, "Analysis of UAV communications in cell-free massive MIMO systems," *IEEE Open J. Commun. Soc.*, vol. 1, pp. 133–147, 2020.

[4] E. Björnson, J. Hoydis, and L. Sanguinetti, *Massive MIMO Networks: Spectral, Energy, and Hardware Efficiency*. Foundations and Trends in Signal Processing Series, Now Publishers, 2018.